Electronic Supplementary Material (ESI) for Dalton Transactions.
This journal is © The Royal Society of Chemistry 2023

Rearrangement of a Ge(II) Aryloxide to Yield a New Ge(II) Oxo-Cluster $[Ge_6(\mu_3\text{-}O)_4(\mu_2\text{-}OC_6H_2\text{-}2,4,6\text{-}Cy_3)_4](NH_3)_{0.5}$: Main Group Aryloxides of Ge(II), Sn(II), and Pb(II) $[M(OC_6H_2\text{-}2,4,6\text{-}Cy_3)_2]_2$ (Cy=Cyclohexyl)

Connor P. McLoughlin,[a] Derrick C. Kaseman,[b,c] James C. Fettinger,[a] and Philip P. Power [a*]

[a]Department of Chemistry, University of California, One Shields Avenue, Davis, California 95616, United States

[b]Nuclear Magnetic Resonance Facility, University of California, One Shields Avenue, Davis, California 95616, United States

[c]Biochemistry and Biotechnology Group, Los Alamos National Laboratory, Los Alamos, New Mexico 87545, United States

Supporting Information

Table of Contents:

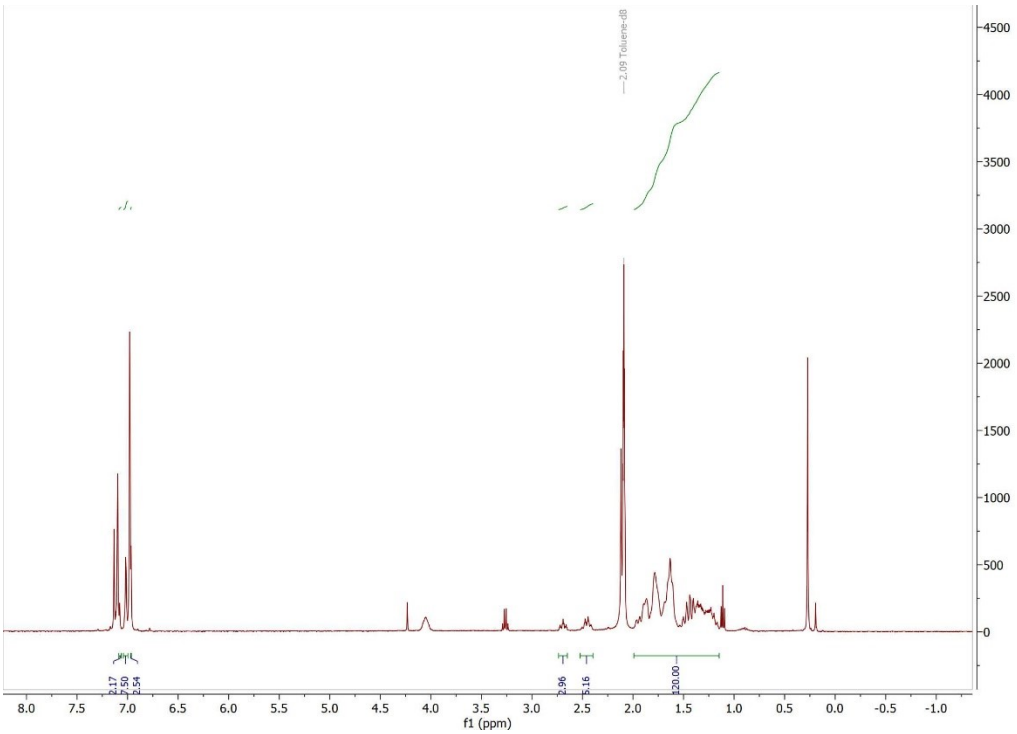

Figure S1. ^{1}H NMR spectrum (25 ^{o}C, C_7D_8, 400 MHz) of $[Ge_6(\mu_3\text{-}O)_4(\mu_2\text{-}OC_6H_2\text{-}2,4,6\text{-}Cy_3)_4](NH_3)_{0.5}$ (**1**).

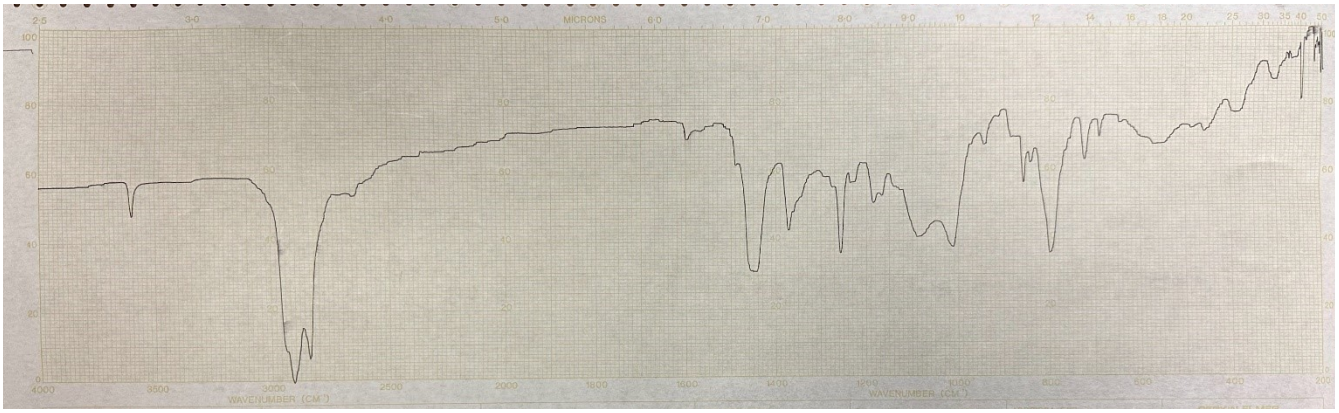

Figure S2. Infrared spectrum of $[Ge_6(\mu_3\text{-}O)_4(\mu_2\text{-}OC_6H_2\text{-}2,4,6\text{-}Cy_3)_4](NH_3)_{0.5}$ (**1**).

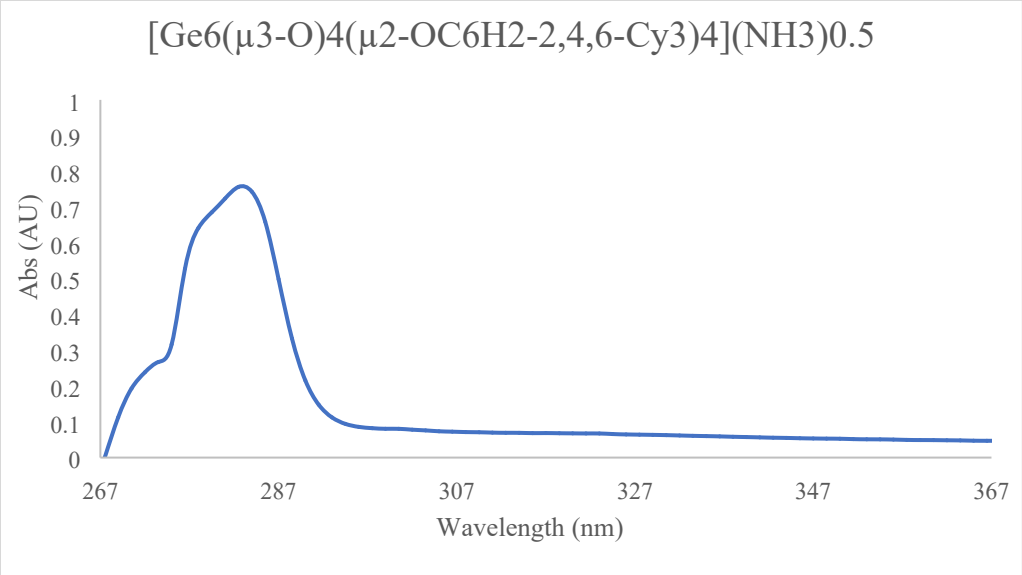

Figure S3. UV-Vis spectrum (73 μM, toluene) of $[Ge_6(\mu_3\text{-}O)_4(\mu_2\text{-}OC_6H_2\text{-}2,4,6\text{-}Cy_3)_4](NH_3)_{0.5}$ (**1**).

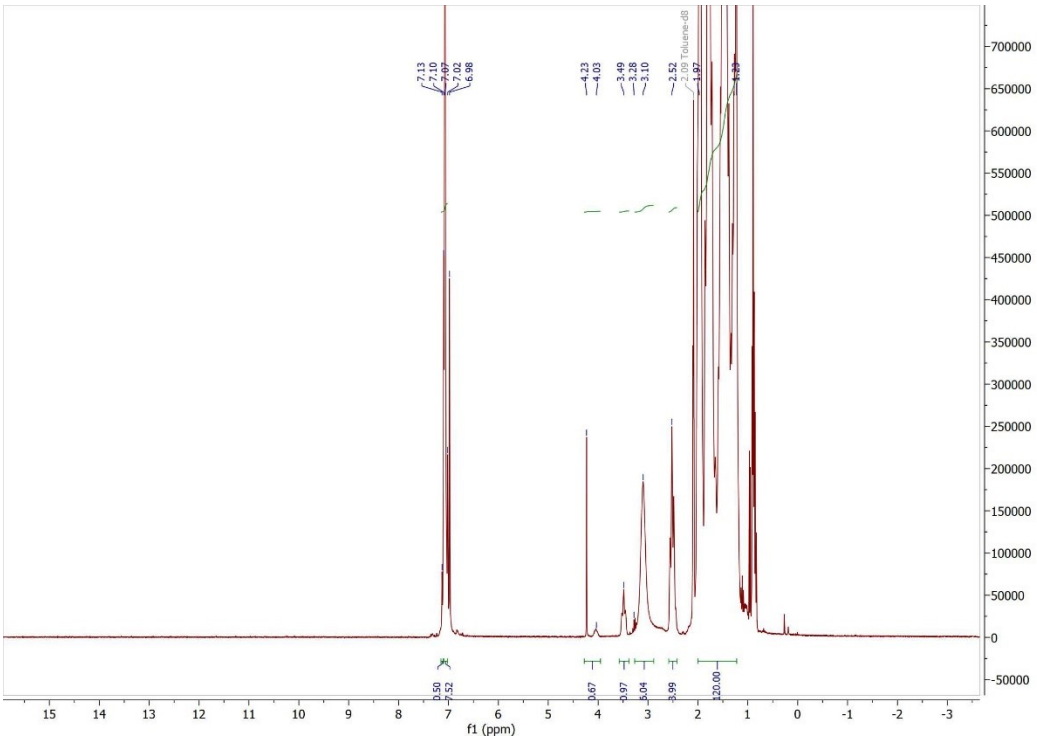

Figure S4. ^1H NMR spectrum (25 °C, C_7D_8, 400 MHz) of $[Ge(OC_6H_2\text{-}2,4,6\text{-}Cy_3)_2]_2$ (**2**).

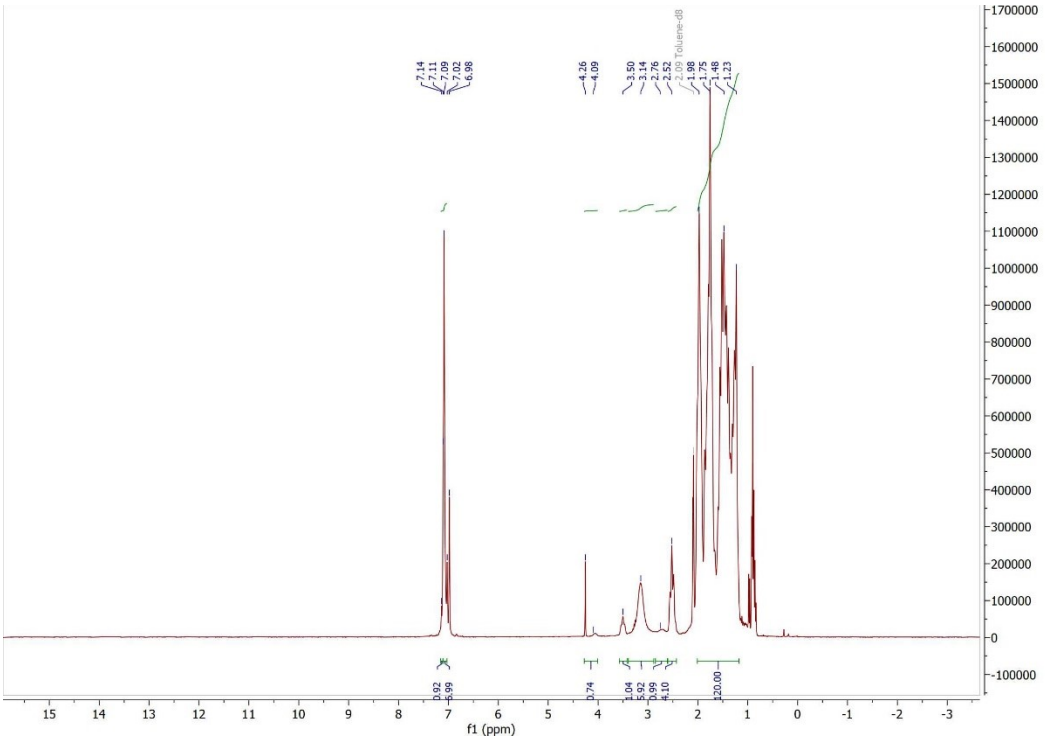

Figure S5. ^{1}H NMR spectrum (11 ^{o}C, C_7D_8, 300 MHz) of $[Ge(OC_6H_2\text{-}2,4,6\text{-}Cy_3)_2]_2$ (**2**).

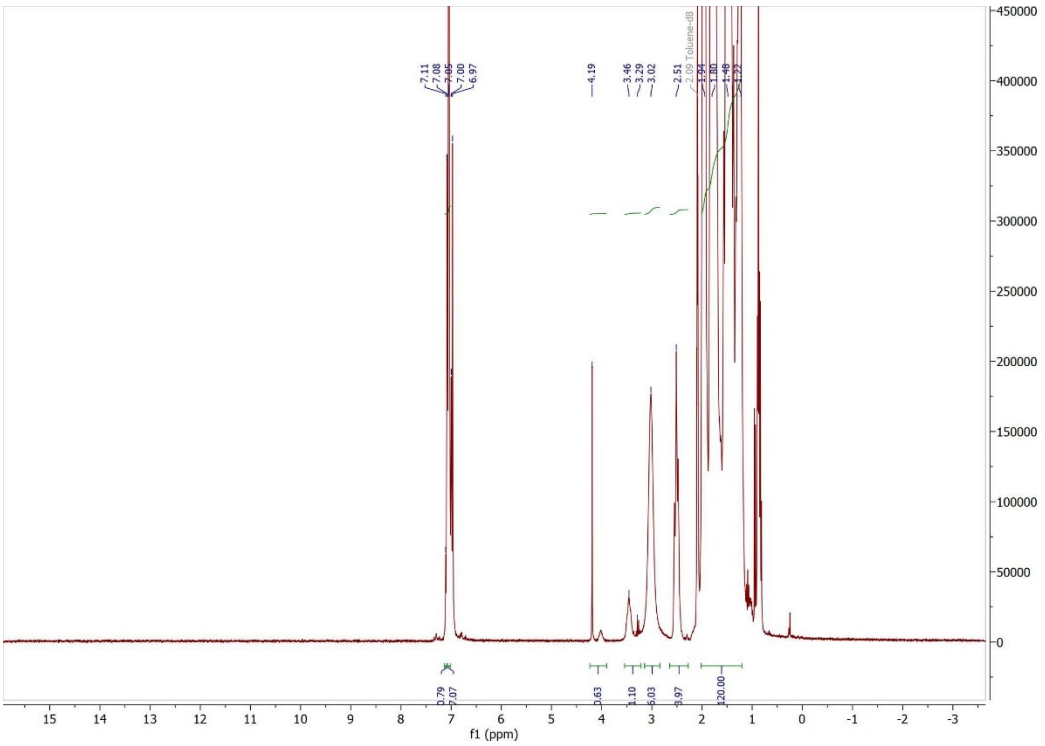

Figure S6. ^{1}H NMR spectrum (55 ^{o}C, C_7D_8, 300 MHz) of $[Ge(OC_6H_2\text{-}2,4,6\text{-}Cy_3)_2]_2$ (**2**).

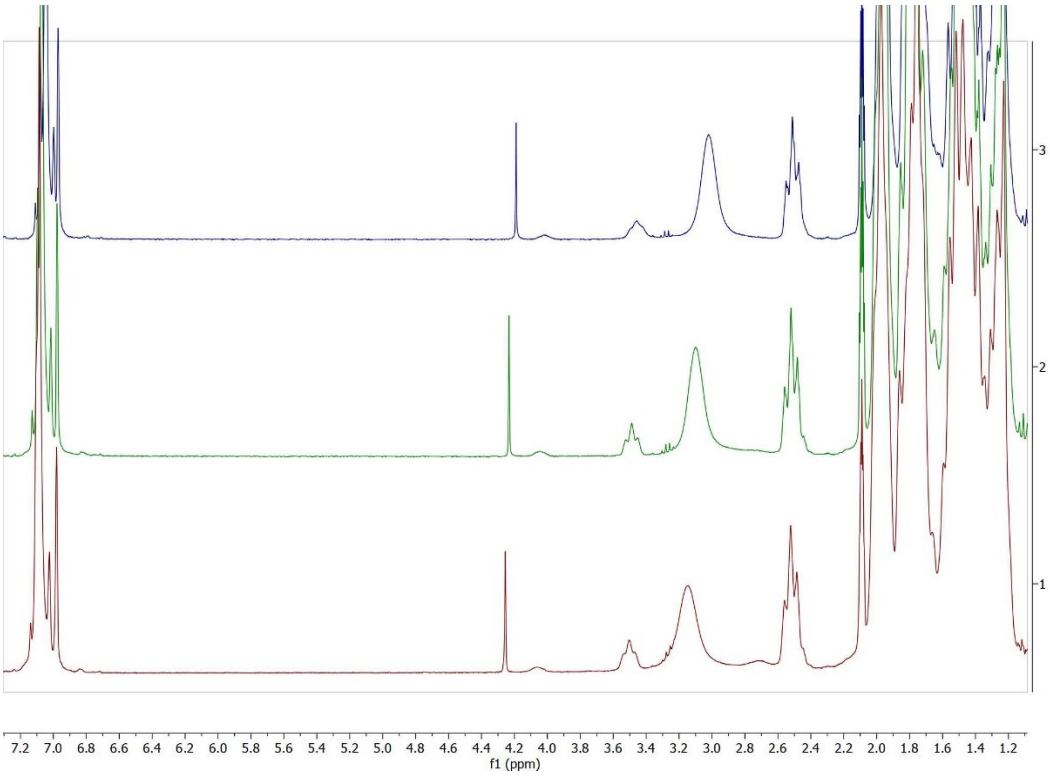

Figure S7. Stacked Variable temperature ^{1}H NMR spectra (11^{o} {bottom}, 25^{o} {middle}, 55 ^{o}C {top}, C_7D_8, 300 MHz) of $[Ge(OC_6H_2\text{-}2,4,6\text{-}Cy_3)_2]_2$ (**2**).

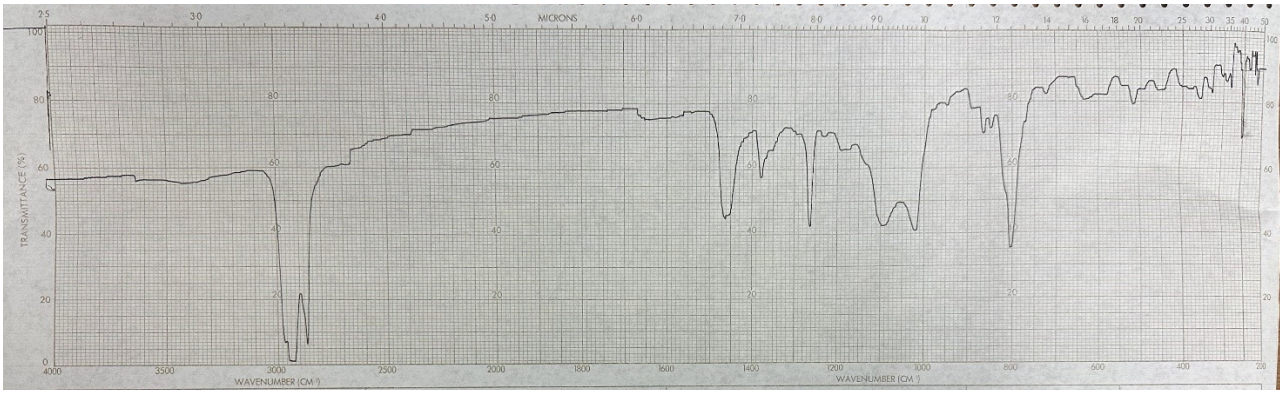

Figure S8. Infrared spectrum (Nujol) of $[Ge(OC_6H_2\text{-}2,4,6\text{-}Cy_3)_2]_2$ (**2**).

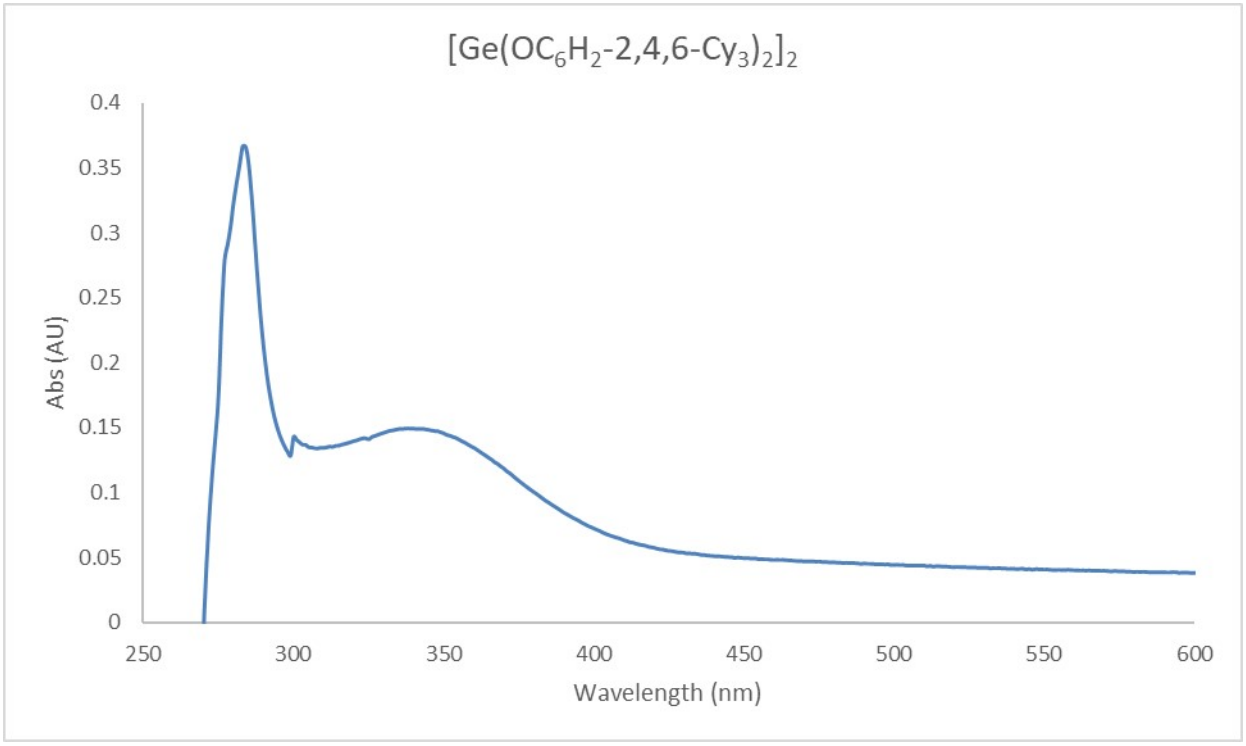

Figure S9. UV-Vis spectrum (46 µM, toluene) of $[Ge(OC_6H_2\text{-}2,4,6\text{-}Cy_3)_2]_2$ (**2**).

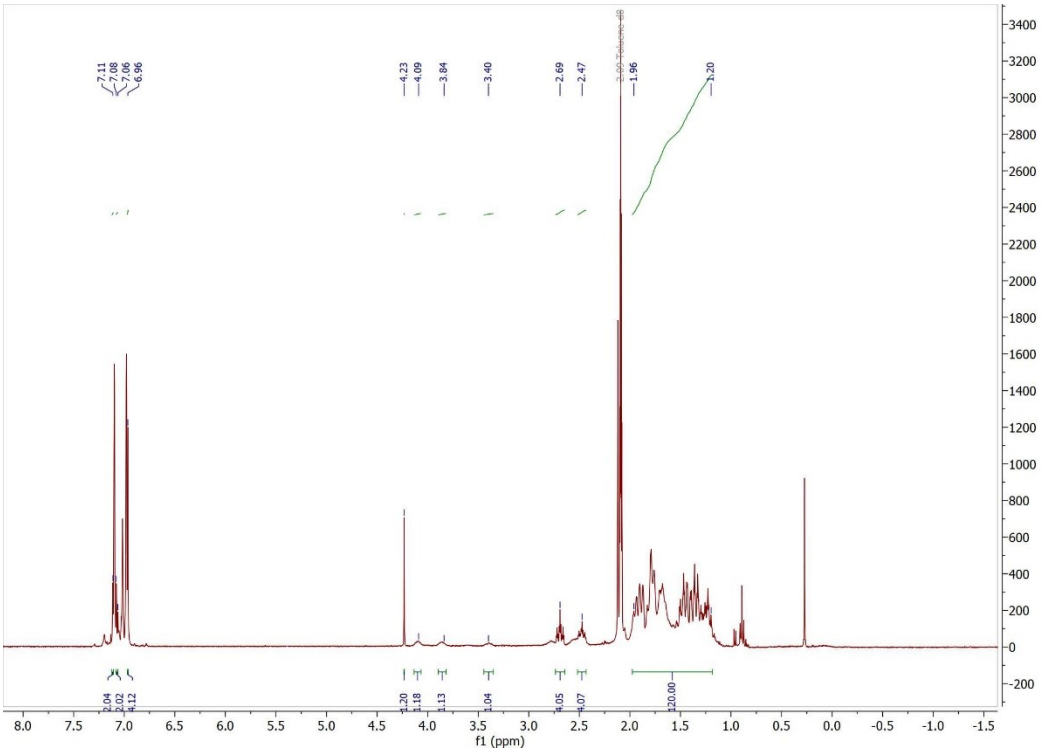

Figure S10. ^{1}H NMR spectrum (25 ^{o}C, C_7D_8, 400 MHz) of $[Sn(OC_6H_2\text{-}2,4,6\text{-}Cy_3)_2]_2$ (**3**).

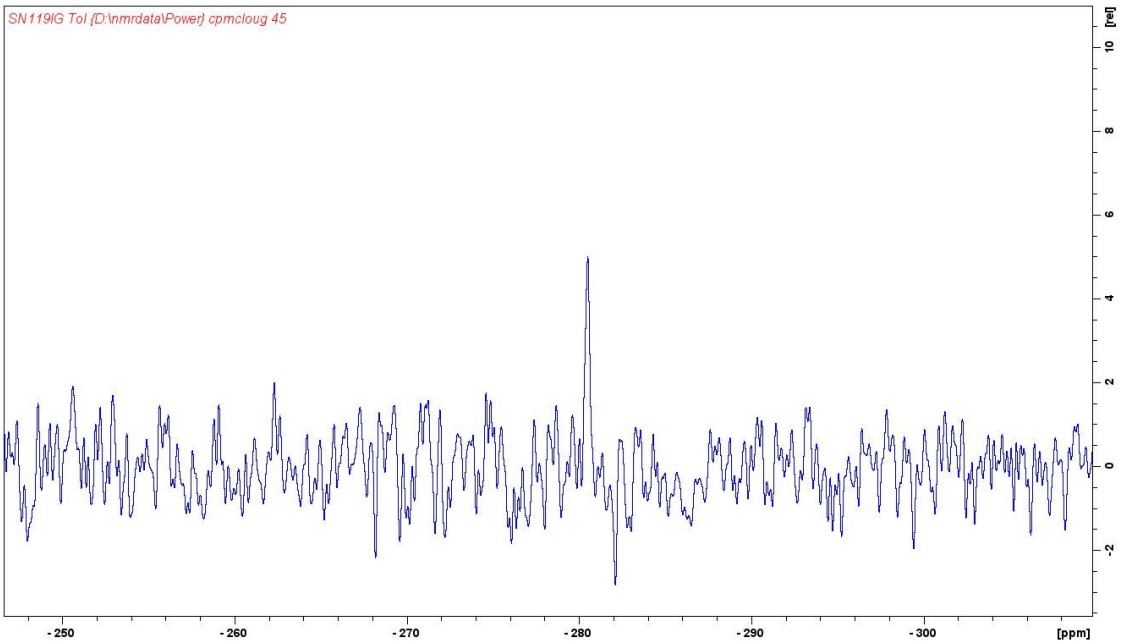

Figure S11. ^{119}Sn NMR spectrum* (25 ^{o}C, C_7D_8, 149.07 MHz) of $[Sn(OC_6H_2\text{-}2,4,6\text{-}Cy_3)_2]_2$ (**3**).

The initial acquisition parameters included a dwell time of 5 ms, recycle delay of 10 ms, and 16,384 FIDs were averaged for an acquisition time of 9.8 ms and a repetition time of 20 ms (total experimental time 15 minutes). The initial 10 ms acquisition time was too short from the long T_2 of the narrow resonance and resulted in truncation of the signal leading to characteristic sinc wiggles and broadening of the ^{119}Sn resonance (FWHM=65 Hz). The new acquisition parameters include 24,576 FIDs, dwell time of 16 µs, recycle delay of 500 ms for an acquisition time of 260 ms and a recycle delay of 760 ms (total experimental time 5 hours). The FWHM of this peak is narrower (38.7 Hz) indicating that the reviewer was correct and that the parameters could be optimized.

Making the initial assumption that $T_2^*=T_2=T_1$ that is generally valid in liquid state NMR, we can estimate from the linewidth that the T_1 of the sample is ~8 ms, indicating that the initial set of parameters was collecting only $1*T_2$ which gives the expected truncation wiggles in the spectrum. However, with the T_1 being very short and only using a 30-degree tip angle, good SNR could be obtained with a fast recycle delay. Fundamentally, the information obtained in both spectra are the same with a single chemical shift at -280.5 ppm. The low signal to noise ratio is easily explained by the low sample concentration due to solubility and the relatively high molecular weight and prevents additional information such as isotopologues from being observed.

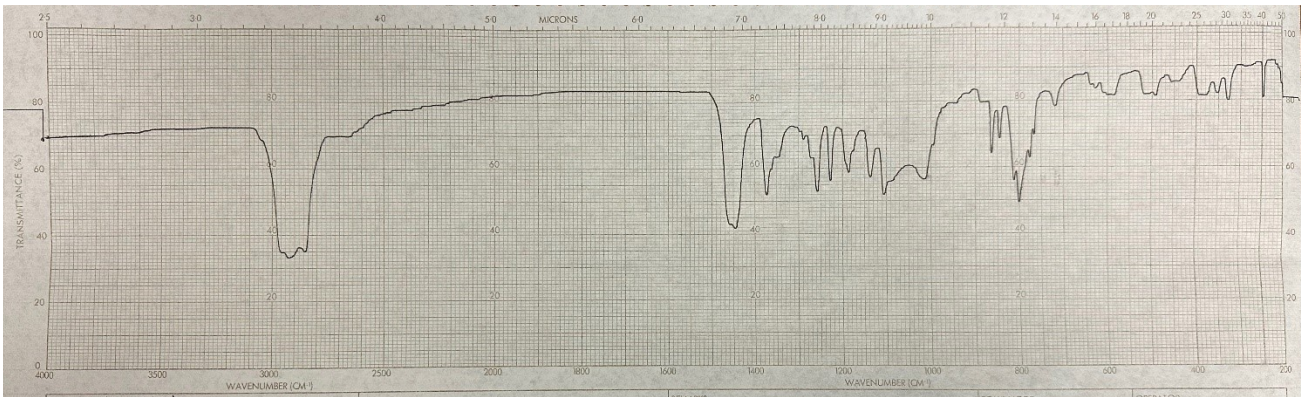

Figure S12. Infrared spectrum (Nujol) of $[Sn(OC_6H_2\text{-}2,4,6\text{-}Cy_3)_2]_2$ (**3**).

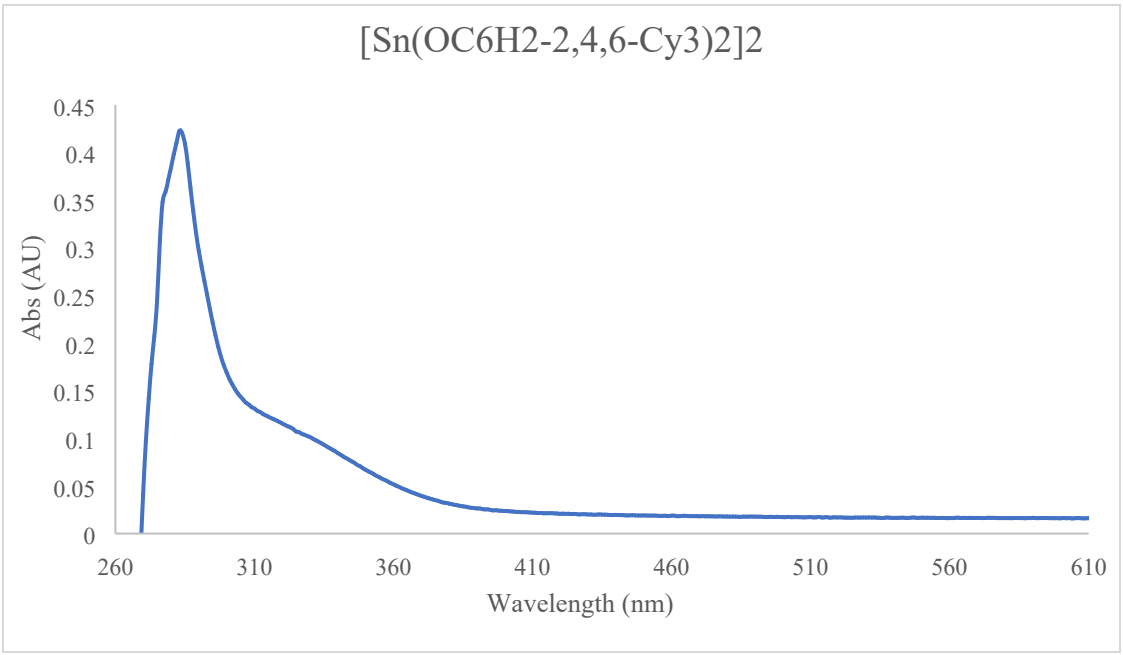

Figure S13. UV-Vis spectrum (53 µM, toluene) of $[Sn(OC_6H_2\text{-}2,4,6\text{-}Cy_3)_2]_2$ (**3**).

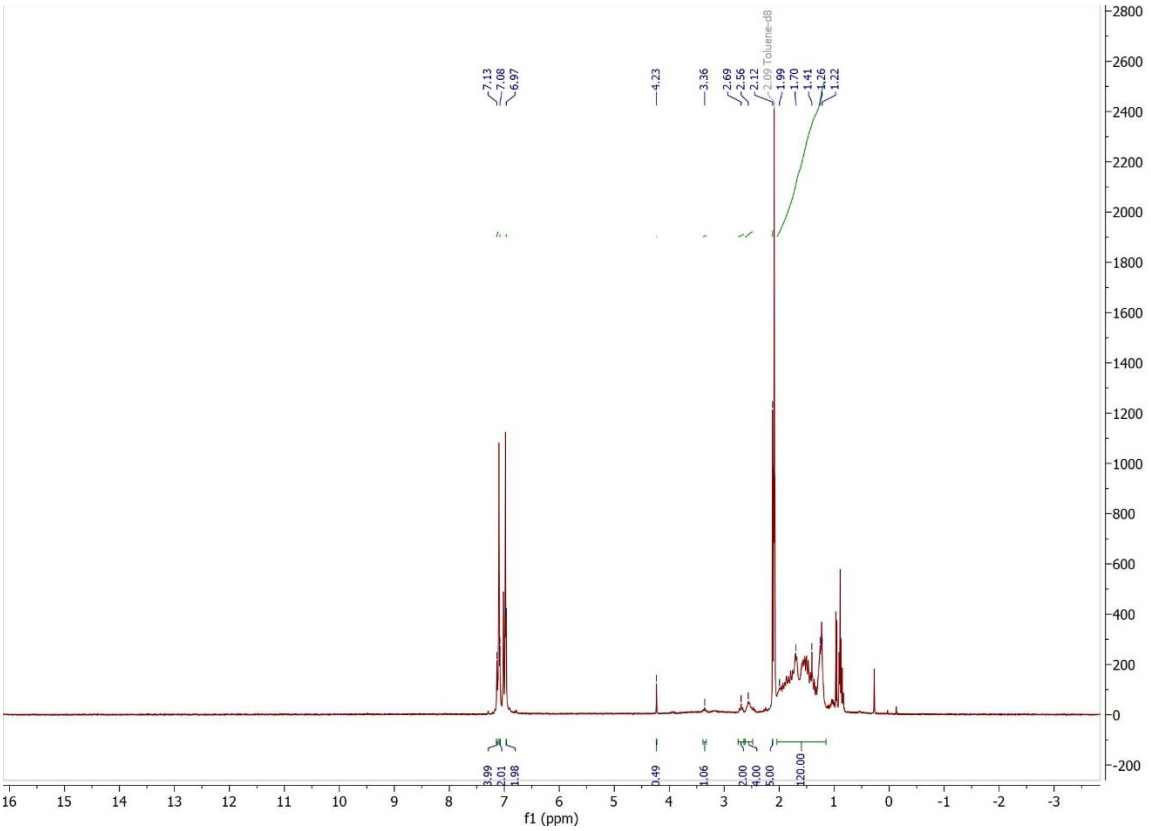

Figure S14. ^{1}H NMR spectrum (25 ^{o}C, C_7D_8, 400 MHz) of $[Pb(OC_6H_2\text{-}2,4,6\text{-}Cy_3)_2]_2$ (**4**).

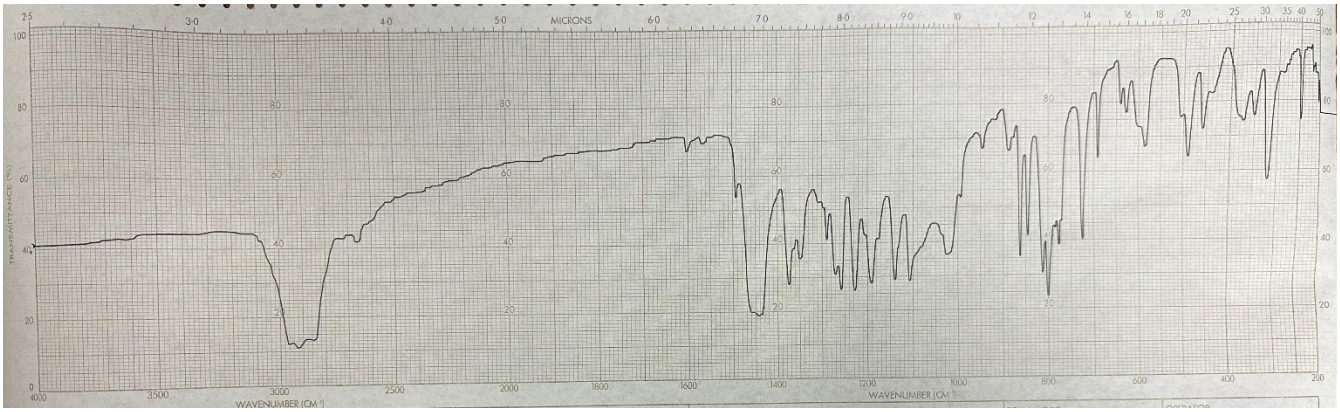

Figure S15. Infrared spectrum (Nujol) of $[Pb(OC_6H_2\text{-}2,4,6\text{-}Cy_3)_2]_2$ (**4**).

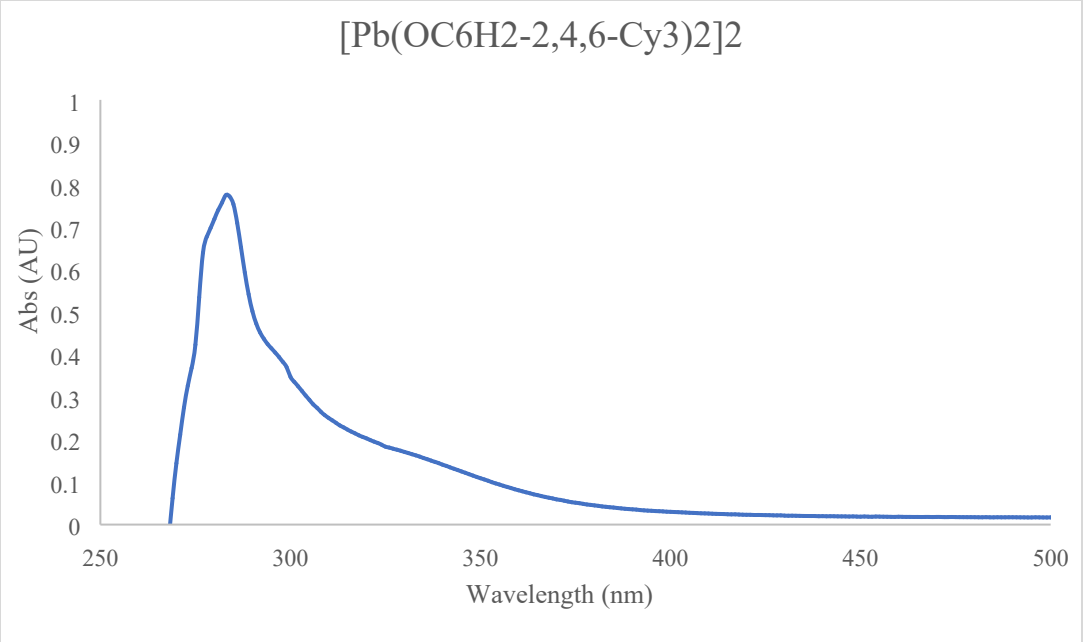

Figure S16. UV-Vis spectrum (25 °C, 50 µM, toluene) of $[Pb(OC_6H_2\text{-}2,4,6\text{-}Cy_3)_2]_2$ (**4**).

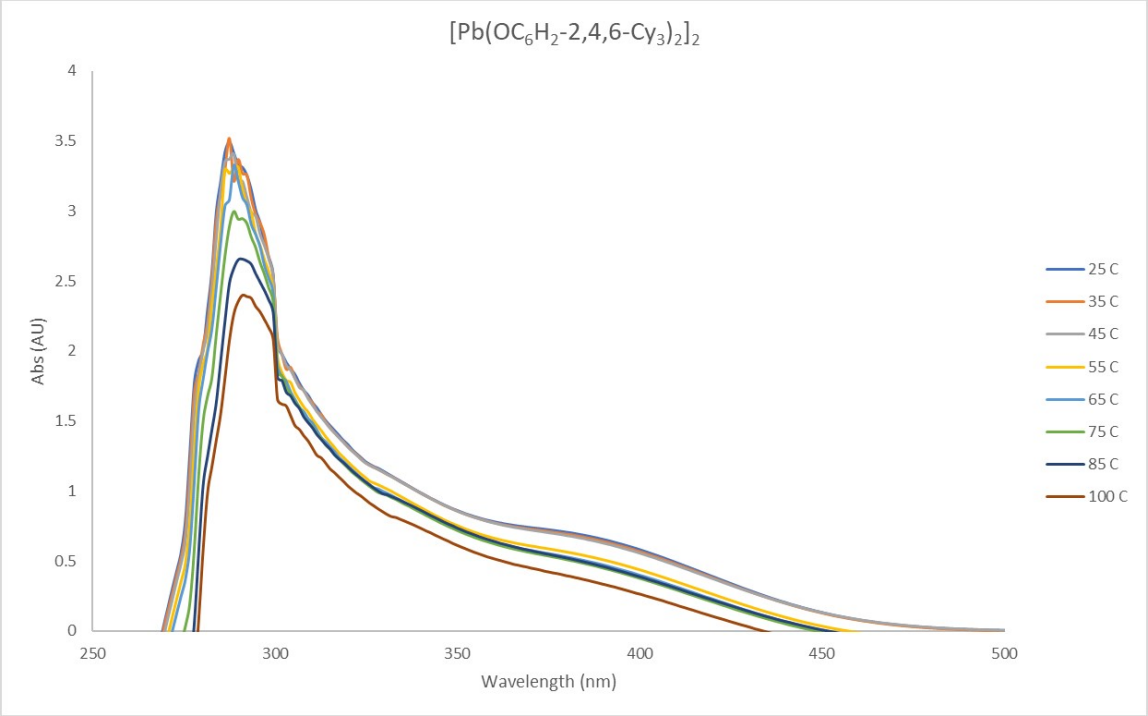

Figure S17. Variable temperature UV-Vis spectra (250 µM, toluene) of $[Pb(OC_6H_2\text{-}2,4,6\text{-}Cy_3)_2]_2$ (**4**).

Table S1. Crystal data and structure refinement for **1**-**4**

	1	**2**	**3**	**4**
Empirical formula	C124 H173.50 Ge6 N0.50 O8	C96 H140 Ge2 O4	C110 H156 O4 Sn2	C96 H140 O4 Pb2
Formula weight	2234.66	1503.31	1779.72	1772.45
Temperature	150(2) K	100(2) K	90(2) K	90(2) K
Wavelength	0.71073 Å	0.71073 Å	0.71073 Å	0.71073 Å
Crystal system	Monoclinic	Monoclinic	Monoclinic	Monoclinic
Space group	C2/c	$P2_1/c$	$P2_1$	$P2_1/n$
Unit cell dimensions	a = 28.917(4) Å	a = 19.3073(12) Å	a = 12.1851(2) Å	a = 18.4668(8) Å
	b = 28.936(4) Å	b = 16.9581(11) Å	b = 26.1606(4) Å	b = 16.8063(6) Å
	c = 29.722(4) Å	c = 31.157(2) Å	c = 15.8166(3) Å	c = 19.1231(8) Å
	a= 90°.	a= 90°.	a= 90°.	a= 90°.
	b= 108.188(4)°.	b= 100.2858(16)°.	b= 107.6338(9)°.	b= 117.133(2)°.
	g = 90°.	g = 90°.	g = 90°.	g = 90°.
Volume	23627(5) Å3	10037.4(11) Å3	4804.94(14) Å3	5281.9(4) Å3
Z	8	4	2	2
Density (calculated)	1.256 Mg/m3	0.995 Mg/m3	1.230 Mg/m3	1.114 Mg/m3
Absorption coefficient	1.560 mm-1	0.641 mm-1	0.571 mm-1	3.223 mm-1
F(000)	9416	3248	1896	1824
Crystal size	0.206 x 0.185 x 0.030 mm3	0.380 x 0.186 x 0.080 mm3	0.340 x 0.201 x 0.079 mm3	0.457 x 0.272 x 0.190 mm3
Crystal color and habit	Colorless Rectangular	Colourless Rectangular	Colorless Rectangular	Yellow Rectangular Block
Diffractometer	Bruker Photon2 CMOS	Bruker Photon2 CMOS	Bruker APEX-II CCD	Bruker APEX-II CCD
Theta range for data collection	1.948 to 25.551°.	1.072 to 27.510°.	1.557 to 27.544°.	1.733 to 25.488°.
Index ranges	-34<=h<=34, -34<=k<=34, -35<=l<=35	-25<=h<=25, -22<=k<=22, -40<=l<=40	-15<=h<=15, -33<=k<=33, -20<=l<=20	-22<=h<=22, -20<=k<=20, -23<=l<=23
Reflections collected	85260	88299	37967	33242
Independent reflections	21934 [R(int) = 0.0997]	23068 [R(int) = 0.0269]	21907 [R(int) = 0.0479]	9776 [R(int) = 0.0484]
Observed reflections (I > 2sigma(I))	16435	17986	17678	6542
Completeness to theta = 25.242°	99.90%	100.00%	100.00%	99.90%
Absorption correction	Semi-empirical from equivalents	Semi-empirical from equivalents	Semi-empirical from equivalents	Semi-empirical from equivalents
Max. and min. transmission	0.4867 and 0.4279	0.8832 and 0.8432	0.9143 and 0.8565	0.4928 and 0.3730
Solution method	SHELXT (Sheldrick, 2015) Acta Cryst., A71, 3-8	SHELXT (Sheldrick, 2015) Acta Cryst., A71, 3-8	SHELXT (Sheldrick, 2015) Acta Cryst., A71, 3-8	SHELXT (Sheldrick, 2015) Acta Cryst., A71, 3-8

Refinement method	SHELXL-2018/3 (Sheldrick, 2018) Full-matrix least-squares on F2	SHELXL-2018/3 (Sheldrick, 2018) Full-matrix least-squares on F2	SHELXL-2018/3 (Sheldrick, 2018) Full-matrix least-squares on F2	SHELXL-2018/3 (Sheldrick, 2018) Full-matrix least-squares on F2
Data / restraints / parameters	21934 / 403 / 1427	23068 / 0 / 919	21907 / 1 / 1036	9776 / 101 / 544
Goodness-of-fit on F2	1.042	1.044	0.995	1.051
Final R indices [I>2sigma(I)]	R1 = 0.0737, wR2 = 0.2012	R1 = 0.0342, wR2 = 0.0846	R1 = 0.0436, wR2 = 0.0731	R1 = 0.0466, wR2 = 0.1086
R indices (all data)	R1 = 0.0984, wR2 = 0.2234	R1 = 0.0470, wR2 = 0.0905	R1 = 0.0623, wR2 = 0.0803	R1 = 0.0795, wR2 = 0.1254
Largest diff. peak and hole	2.549 and -0.865 e.Å-3	1.006 and -0.480 e.Å-3	0.570 and -0.461 e.Å-3	1.156 and -0.713 e.Å-3

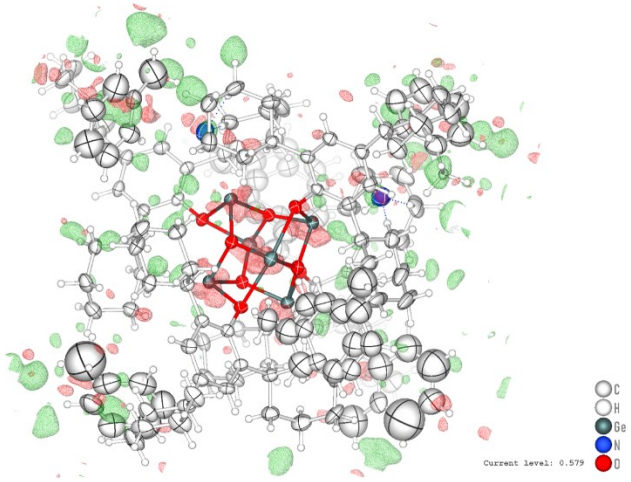

Figure S18. Electron density map for **1** and comments.

There is minimal residual electron density around one of the nitrogen atoms. Many atoms are not seen in residual electron density maps when dealing with light atoms that rotate freely. Hydrogen is the lightest atom and is therefore the most difficult to locate whenever it has any form of unrestricted motion, as it does in the case of compound 1. We also observe an υN-H vibrational mode in the IR spectrum of compound 1 confirming the presence of hydrogen atoms around the nitrogen atoms, despite the difficulty in locating them crystallographically.

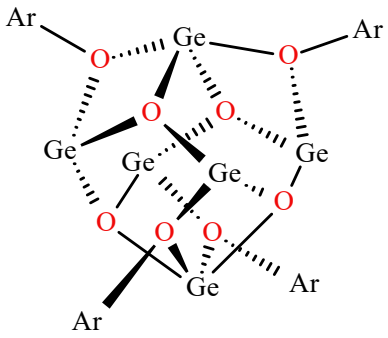

Ar = -C_6H_2-2,4,6-Cy_3 (Cy=Cyclohexyl)

Figure S19. Line drawing demonstrating the connectivity of the core atoms in compound **1**.